Inorg. Chem. **2003**, *42*, 6106–6113

Ferro- and Ferrimagnetic Chains of hin-Bridged Copper(II) and Manganese(II) and hnn-Bridged Manganese(II) Complexes (hin = 4,4,5,5-Tetramethylimidazolin-1-oxyl; hnn = 4,4,5,5-Tetramethylimidazolin-1-oxyl 3-Oxide)

Tomoaki Ise,[†] Takayuki Ishida,* Daisuke Hashizume,[‡] Fujiko Iwasaki, and Takashi Nogami

Department of Applied Physics and Chemistry, The University of Electro-Communications, Chofu, Tokyo 182-8585, Japan

Received April 14, 2003

We have exploited potential utility of 4,4,5,5-tetramethylimidazolin-1-oxyl (hin) and 4,4,5,5-tetramethylimidazolin-1-oxyl 3-oxide (hnn) as μ-1,4 and μ-1,5 bridging ligands, respectively, carrying an unpaired electron in development of metal–radical hybrid magnets. X-ray diffraction measurements of [Cu(hfac)$_2$hin] (**1**), [Mn(hfac)$_2$hin] (**2**), and [Mn(hfac)$_2$hnn] (**3**) revealed one-dimensional metal–radical alternating chain structures, where hfac denotes 1,1,1,5,5,5-hexafluoropentane-2,4-dionate. Magnetic measurements of **1** indicate the presence of intrachain ferromagnetic coupling between copper and radical spins. The magnetic exchange parameter was estimated as $2J/k = 56.8$ K based on an $S = {}^1/_2$ equally spaced ferromagnetic chain model ($H = -2J\sum S_i \cdot S_{i+1}$). This ferromagnetic interaction can be explained in terms of the axial coordination of the hin nitrogen or oxygen to Cu^{II}. The $\chi_m T$ value of **2** and **3** increased on cooling, and the magnetic data could be analyzed by Seiden's ferrimagnetic chain model, giving $2J/k = -325$ and -740 K, respectively. The antiferromagnetic interaction of **2** and **3** can be attributed to orbital overlap between the manganese and the oxygen or nitrogen magnetic orbitals. The exchange interactions between Cu–hin and Mn–hnn are larger than those of typical Cu– and Mn–nitronyl nitroxide complexes, indicating that the choice of small ligands is a promising strategy to bestow strong exchange interaction. Compound **3** became a ferrimagnet below 4.4 K, owing to ferromagnetic coupling among the ferrimagnetic chains.

Introduction

The design and synthesis of molecule-based magnetic materials is one of the major subjects of materials science. There have been ample examples of alternating one-dimensional complexes containing nitronyl nitroxide radicals (Chart 1) and metal hfac salts[1] in pursuit of metal−radical hybrid magnets (hfac denotes 1,1,1,5,5,5-hexafluoropentane-2,4-dionate). The ferro- and ferrimagnetic couplings within the chain structure have been well characterized, depending on the symmetry of d-magnetic orbitals on the metal ions and also on the mutual geometry of the ligating oxygen atoms and metal ions (equatorial/axial positions of the metal ions, trans/cis zigzag structures of the chains, etc.). The imino nitroxide radicals are also well-known[2] and the imino nitrogen atom is potentially available for coordination to metal ions.[3] However, there has been no report on one- or higher-dimensional complexes containing imino nitroxide bridges.

Chart 1. Structural Formulas

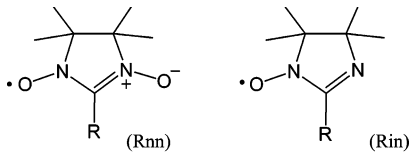

* Corresponding author. Phone: +81-424-43-5490. Fax: +81-424-43-5501. E-mail address: ishi@pc.uec.ac.jp.

[†] Present address: Department of Materials Science, Graduate School of Science, Osaka City University, Sumiyoshi-ku, Osaka 558-8585, Japan.

[‡] Present address: Molecular Characterization Division, The Institute of Physical and Chemical Research (RIKEN), Hirosawa, Wako 351-0198, Japan.

(1) Caneschi, A.; Gatteschi, D.; R. Sessoli, R. *Acc. Chem. Res*. **1989**, *22*, 392. Caneschi, A.; Gatteschi, D.; Rey, P. *Prog. Inorg. Chem.* **1991**, *39*, 33. Caneschi, A.; Gatteschi, D.; Renard, J. P.; Rey, P.; Sessoli, R. *Inorg. Chem.* **1989**, *28*, 1976. Caneschi, A.; Gatteschi, D.; Renard, J. P.; Rey, P.; Sessoli, R. *J. Am. Chem. Soc*. **1989**, *111*, 785.

(2) Ullman, E. F.; Call, L.; Osiecki, J. H. *J. Org. Chem.* **1970**, *35*, 3623.

10.1021/ic034392x CCC: $25.00
Published on Web 08/23/2003

We assume that the choice of small ligands and anions is crucial in order to bestow strong exchange interaction on magnetic materials. Furthermore, imino nitroxides can serve as a μ-1,4 bridge, which is shorter than nitronyl nitroxides widely used as a μ-1,5 bridge. We chose 4,4,5,5-tetramethylimidazolin-1-oxyl (hin) and 4,4,5,5-tetramethylimidazolin-1-oxyl 3-oxide (hnn) (R = H in Chart 1) as the smallest ligands in the imino and nitronyl nitroxide families.[2] Although the isolation of hin was claimed to be difficult because of its instability,[2] complexation affords a chance to purify and characterize hin compounds. Actually, $[CdCl_2(hin)_4]$ was characterized as the first hin complex.[4] We also reported two mononuclear complexes, $[M(hfac)_2(hin)_2]$ (M = Cu, Mn),[5] in which the imino nitrogen atom is coordinated to the metal ion, whereas the nitroxide oxygen atom remains uncoordinated. We report here the crystal structure and magnetic properties of $[M(hfac)_2hin]$ (M = Cu (**1**), Mn(**2**)) and $[Mn(hfac)_2hnn]$ (**3**) as one-dimensional complexes. These hin compounds are the first examples which possess ferro- or ferrimagnetic infinite chain structures containing imino nitroxide bridges.

Experimental Section

Materials. 4,4,5,5-Tetramethylimidazolin-1-oxyl (hin) was prepared according to the literature method[2] with a slight modification.[5]

$[Cu(hfac)_2hin]$ (1). After the solutions of hin (100 mg, 0.71 mmol) in dry ether (3 mL) and of dehydrated $Cu(hfac)_2$ (1.0 g, 2.1 mmol) in dry ether (3 mL) were mixed, the combined solution was allowed to stand in a cool and dark place for 1 day, and dark-brown crystals of **1** were precipitated. $[Mn(hfac)_2hin]$ (**2**) was synthesized in a similar manner. Unfortunately, **2** was obtained only as a fine polycrystalline form. When the molar ratio of starting materials was 1/1, we obtained only mononuclear complexes $[M(hfac)_2(hin)_2]$.[5]

$[Mn(hfac)_2hnn]$ (3). Solutions of dehydrated $Mn(hfac)_2$ (300 mg, 0.64 mmol) in a mixed solvent of dry *n*-heptane (70 mL) and ether (5 mL) and of hnn (100 mg, 0.64 mmol) in dry CH_2Cl_2 (10 mL) were combined, then the solution was allowed to stand in a cool and dark place for 1 day, and dark-purple crystals of $[Mn(hfac)_2hnn]$ were precipitated.

Elemental analysis (C, H, N) of these complexes on a Fisons EA-1108 by a usual combustion method revealed that the metal/radical ratios were 1/1 for **1**−**3**. Anal. Calcd for $C_{17}H_{15}N_2O_5F_{12}Cu_1$ (**1**): C, 32.99; H, 2.44; N, 4.53. Found: C, 32.37; H, 1.87; N, 4.62. Calcd for $C_{17}H_{15}N_2O_5F_{12}Mn_1$ (**2**): C, 33.46; H, 2.48; N, 4.59. Found: C, 33.61; H, 2.55; N, 4.09. Calcd for $C_{17}H_{15}N_2O_6F_{12}Mn_1$ (**3**): C, 32.64; H, 2.41; N, 4.47. Found: C, 31.98; H, 2.78; N, 4.69.

X-ray Crystallographic Analysis. Single-crystal diffraction data of **1** and **3** were collected on a Rigaku Raxis-Rapid diffractometer with graphite-monochromated Mo Kα radiation at 93 and 100 K, respectively. Numerical absorption correction was used. Full-matrix least-squares methods were applied using all of the unique diffraction data. The structure of **1** was solved by a direct method (SIR97[6]) and refined by a full-matrix least-squares method with the SHELXL97[7] program. Anisotropic temperature factors were applied for non-hydrogen atoms except for C6 and C7. Since C6 and C7 are very close to symmetry relatives in a disordered model, application of anisotropic temperature factors for the atoms brings about large parameter interaction and leads to unrealistic structures. Hydrogen atoms were refined by use of the riding model. The structure of **3** was directly solved by a heavy-atom Patterson method in the teXsan program package.[8] The thermal displacement parameters of all non-hydrogen atoms were refined anisotropically, and those of hydrogen atoms were done isotropically. A conformationally disordered model for the C34 trifluoromethyl group was applied to improve the refinement, and the optimized occupancy ratio was 0.68/0.32. Selected crystallographic data of **1** and **3** are listed in Table 1.[9]

Table 1. Selected X-ray Crystallographic Data of $[Cu(hfac)_2hin]$ (**1**) and $[Mn(hfac)_2hnn]$ (**3**)

compound	$[Cu(hfac)_2hin]$ (**1**)	$[Mn(hfac)_2hnn]$ (**3**)
formula	$C_{17}H_{15}N_2O_5F_{12}Cu_1$	$C_{17}H_{15}N_2O_6F_{12}Mn_1$
fw	618.84	626.23
crystal system	orthorhombic	monoclinic
space group	*Pbcn*	$P2_1/a$
a/Å	16.859(1)	17.8592(9)
b/Å	10.835(6)	12.4360(5)
c/Å	12.830(1)	21.702(1)
β/deg	90	103.486(1)
V/Å^3	2343.7(3)	4687.1(4)
Z	4	8
D_{calc}/g cm^{-3}	1.75	1.77
T/K	93	100
$R(I > 2\sigma(I))^a$	0.046	0.068
R_w (all data)^b	0.108	0.200

^{a} $R = \sum(||F_o| - |F_c||)/\sum|F_o|$. ^{b} $R_w = [\sum w(|F_o| - |F_c|)^2/\sum w|F_c|^2]^{1/2}$.

Magnetic measurements. Magnetic properties of polycrystalline specimens were measured on a Quantum Design MPMS SQUID magnetometer equipped with a 7 T coil in a temperature range down to 1.8 K. The magnetic responses were corrected with diamagnetic blank data of the sample holder obtained separately. The diamagnetic contribution of the sample itself was estimated from Pascal's constants. Ac magnetic susceptibility was measured on a Quantum Design PPMS ac/dc magnetometer in a temperature range down to 2.0 K.

Results

Crystal Structures. Figure 1a shows a repeating unit of **1**, and a half of the unit is crystallographically independent. The hin ligand lies close to the 2-fold axis at (0, y, $^1/_4$) and displays a 2-fold disorder about that axis. One of the disordered parts having a Cu−N2 bond is omitted in Figure 1a, but Cu−O3 and Cu−N2 bonds are completely disordered with the 50% occupancy each at every Cu axial position. The Cu atom is located on a crystallographic inversion center

(3) Luneau, D.; Rey, P.; Laugier, J.; Fries, P.; Caneschi, A.; Gatteschi, D.; Sessoli, R. *J. Am. Chem. Soc.* **1991**, *113*, 1245. Oshio, H.; Watanabe, T.; Ohto, A.; Ito, T.; Masuda, H. *Inorg. Chem.* **1996**, *35*, 472. Cogne, A.; Laugier, J.; Luneau, D.; Rey, P. *Inorg. Chem.* **2000**, *39*, 5510. Yamamoto, Y.; Suzuki, T.; Kaizaki, S. *J. Chem. Soc., Dalton Trans.* **2001**, 2943. Tsukuda, T.; Suzuki, T.; Kaizaki, S. *J. Chem. Soc., Dalton Trans.* **2002**, 1721. Ichimura, T.; Doi, K.; Mitsuhashi, C.; Ishida, T.; Nogami, T. *Polyhydron* **2003**, *22*, 2557.
(4) Ise, T.; Ishida, T.; Nogami, T. *Mol. Cryst. Liq. Cryst.* **2002**, *379*, 147.
(5) Ise, T.; Ishida, T.; Nogami, T. *Bull. Chem. Soc. Jpn.* **2002**, *75*, 2468.
(6) Altomare, A.; Burla, M. C.; Camalli, M.; Cascarano, G.; Giacovazzo, C.; Guagliardi, A.; Moliterni, A. G. G.; Polidori, G.; Spagna, R. *J. Appl. Crystallogr.* **1999**, *32*, 115.
(7) Sheldrick, G. M. *SHELXL97*; University of Göttingen: Göttingen, Germany, 1997.
(8) *teXsan: crystal structure analysis package*; Molecular Structure Corp.: The Woodlands, TX, 1985, 1999.
(9) The structural parameters and magnetic exchange parameters of **1** and **2** in this article are more refined and accordingly more reliable than those preliminarily reported. Ise, T.; Ishida, T.; Nogami, T. *Synth. Met.* **2003**, *137*, 1281.

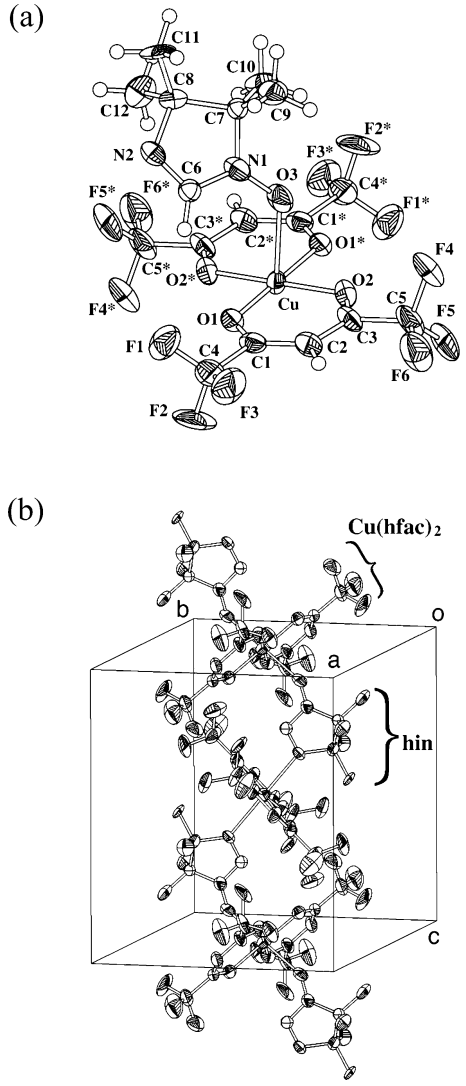

Figure 1. (a) ORTEP view of a repeating unit of [Cu(hfac)$_2$hin] (**1**) at the 50% probability level. Only one of two disordered hin configurations is shown. Symmetry operation code for asterisk (*) is $-x, -y, -z$. (b) Chain structure of **1**. Hydrogen atoms are omitted for the sake of clarity.

Table 2. Selected Bond Distances (Å) and Angles (deg) for [Cu(hfac)$_2$hin] (**1**)

Cu−O1	1.974(2)	Cu−O2	1.938(2)
Cu−O3	2.286(5)	Cu−N2	2.405(7)
C6−N1	1.371(7)	C6−N2	1.274(8)
N1−O3	1.280(7)		
O1−Cu−O2	92.07(9)	O1−Cu−O3	85.10(1)
O2−Cu−O3	98.48(1)	N1−O3−Cu	124.8(5)

at (0, 0, 0). Those symmetry operations generate a one-dimensional structure, in which the hin ligands bind the Cu atoms, and the resultant repeating motifs of hin−Cu(hfac)$_2$ are arranged in a trans zigzag manner as shown in Figure 1b.

Table 2 summarizes selected bond distances and angles for **1**. The octahedra of both copper centers are severely distorted with the axial Cu−O3 and Cu−N2 bonds much longer than the equatorial ones: 2.286(5) and 2.405(7) Å vs 1.974(2) and 1.938(2) Å. The bond length of Cu−O3 is slightly shorter than the typical distances of Cu−O in other nitronyl nitroxide radical complexes.[1] The hin plane is located

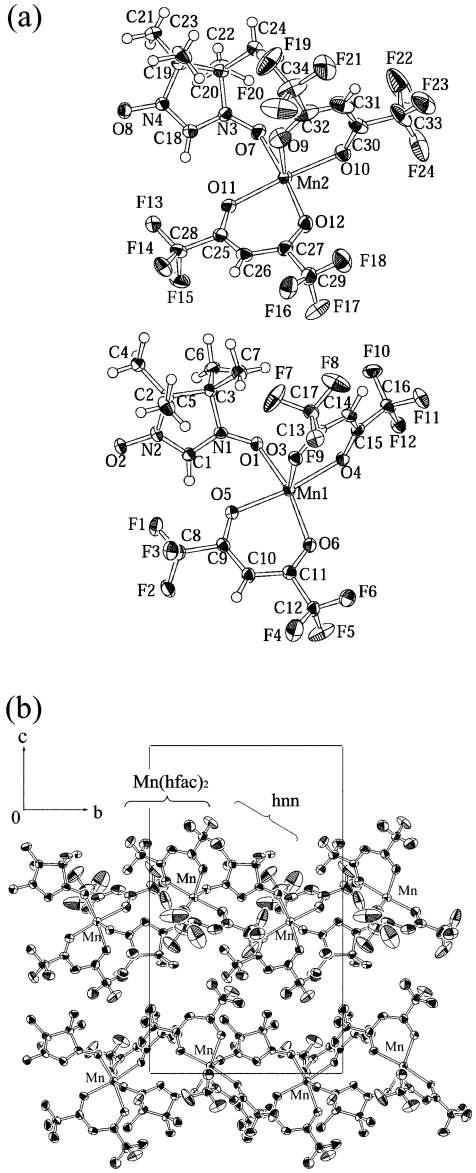

Figure 2. (a) ORTEP view of two independent repeating units of [Mn(hfac)$_2$hnn] (**3**) at the 50% probability level. Only major conformation is shown for a disordered trifluoromethyl group (C34F19F20F21). (b) Chain structures of **3**. Hydrogen atoms are omitted for the sake of clarity.

on a staggered position with respect to the equatorial Cu−O bonds, as indicated by the torsion angle O1−Cu−O3−N1 of 119.5°. The axial O3 and N2 atoms are deviated by only about 10° from the normal to the basal coordination plane. This geometry brings about almost orthogonal arrangement of the magnetic copper $3d_{x^2-y^2}$ orbital and the hin oxygen or nitrogen $2p_z$ orbital. The dihedral angle between two neighboring Cu basal planes is 88.2° in a chain.

Since **2** did not afford single crystals suitable for the X-ray crystal structure analysis, we can report only the cell constants of **2**. The *a*, *b*, and *c* lengths are 15.69(7), 11.65(4), and 13.6(2) Å, respectively, in an orthorhombic crystal system at 296 K. The same crystal system and similar *a*, *b*, and *c* lengths found in **1** and **2** strongly suggest that they are isomorphous.

Figure 2a shows the repeating units of **3**. There are two crystallographically independent hnn−Mn(hfac)$_2$ moieties in

Table 3. Selected Bond Distances (Å) and Angles (deg) for [Mn(hfac)$_2$hnn] (**3**)[a]

Mn1−O1	2.149(2)	Mn2−O7	2.145(3)
Mn1−O2#	2.149(3)	Mn2−O8§	2.142(3)
Mn1−O3	2.149(3)	Mn2−O9	2.147(4)
Mn1−O4	2.150(3)	Mn2−O10	2.122(3)
Mn1−O5	2.152(3)	Mn2−O11	2.151(3)
Mn1−O6	2.164(3)	Mn2−O12	2.163(3)
O1−Mn1−O2#	86.4(1)	O7−Mn2−O8§	87.9(1)
O1−Mn1−O3	95.1(1)	O7−Mn2−O9	87.3(1)
O1−Mn1−O4	88.03(9)	O7−Mn2−O10	93.5(1)
O1−Mn1−O5	85.25(9)	O7−Mn2−O11	91.0(1)
O1−Mn1−O6	165.8(1)	O7−Mn2−O12	173.1(1)
O2#−Mn1−O3	168.1(1)	O8§−Mn2−O9	170.1(1)
O2#−Mn1−O4	85.7(1)	O8§−Mn2−O10	87.8(1)
O2#−Mn1−O5	99.0(1)	O8§−Mn2−O11	91.6(1)
O2#−Mn1−O6	87.2(1)	O8§−Mn2−O12	95.5(1)
O3−Mn1−O4	82.6(1)	O9−Mn2−O10	83.9(1)
O3−Mn1−O5	92.9(1)	O9−Mn2−O11	97.1(1)
O3−Mn1−O6	93.8(1)	O9−Mn2−O12	90.2(1)
O4−Mn1−O5	171.5(1)	O10−Mn2−O11	175.4(1)
O4−Mn1−O6	104.09(9)	O10−Mn2−O12	92.4(1)
O5−Mn1−O6	83.28(9)	O11−Mn2−O12	83.2(1)

[a] Symmetry operation codes: #, $^3/_2 - x$, $-^1/_2 + y$, $1 - z$; §, $^3/_2 - x$, $-^1/_2 + y$, $2 - z$.

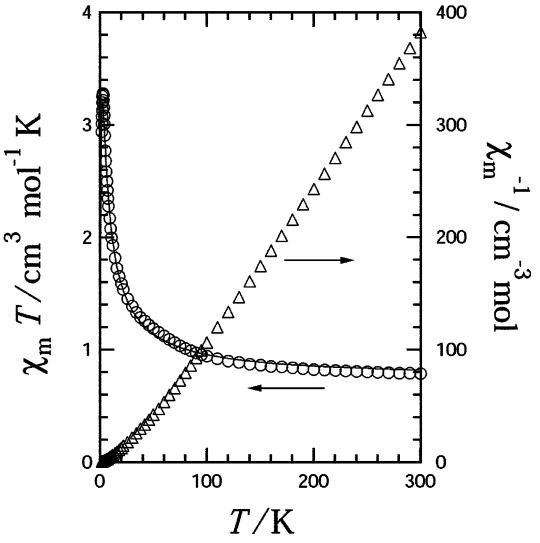

Figure 3. Temperature dependence of the product $\chi_m T$ (○) and χ_m^{-1} (△) measured at 5000 Oe for [Cu(hfac)$_2$hin] (**1**). A solid line represents the theoretical curve based on an $S = ^1/_2$ ferromagnetic chain model.

a unit cell of **3**, but they are practically identical. Each Mn^{II} ion is hexacoordinated by four oxygen atoms of two hfac molecules and by two oxygen atoms of two different hnn radicals. The bond lengths of Mn−O(hnn) are 2.149(2) and 2.149(3) Å for one motif and 2.145(3) and 2.142(3) Å for another. Since the octahedral Mn^{II} ion has a d-electron configuration of $(t_{2g})^3(e_g)^2$, orbital overlaps between the magnetic orbitals of Mn dπ and hnn π^* should be substantial, giving antiferromagnetic interaction. Table 3 summarizes selected bond distances and angles of **3**. Figure 2b shows the linear cis chains of **3**; two hnn oxygen atoms are coordinated in a cis configuration with the O(hnn)−Mn−O(hnn) angles of 86.4(1)° and 87.9(1)°. There are two independent chains running along the *b* axis, which are arrayed alternatively.

Magnetic Properties. The temperature dependence of $\chi_m T$ and χ_m^{-1} measured at 5000 Oe for **1** is shown in Figure 3.

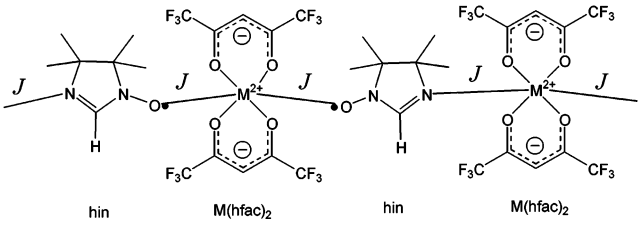

Figure 4. The schematic view of the chain structure of [M(hfac)$_2$hin]. The exchange interaction *J* is defined as an averaged value of M−O and M−N interactions.

The $\chi_m T$ value of **1** is 0.78 cm^3 mol^{-1} K at 300 K, which is slightly larger than the calculated value of 0.75 cm^3 mol^{-1} K for a noncoupled system ($g = 2.0$). A positive Weiss temperature was obtained for **1** from the Curie−Weiss equation $\chi = C/(T - \theta)$ with $C = 0.732$ cm^3 mol^{-1} K and $\theta = 21.9$ K. This finding implies that ferromagnetic interaction is dominant in **1**. Upon cooling, the $\chi_m T$ values increased to a maximum value of 3.28 cm^3 mol^{-1} K at 2.8 K and then decreased. The maximum value is much larger than those of $S = 1$ (1.0 cm^3 mol^{-1} K) due to an expected high-spin repeating unit for **1**, indicating that the ferromagnetic interaction is operative infinitely along the chain structure. The magnetic couplings through Cu−O and Cu−N bonds are expected to be different. However, because of the highly disordered hin orientations, the magnetic exchange coupling in **1** can be described with an averaged parameter *J* (Figure 4).

The experimental data were analyzed by using an $S = ^1/_2$ ferromagnetic chain model[10] (eq 1) for **1** with the Hamiltonian $H = -2J\sum S_i \cdot S_{i+1}$, where all symbols have their usual meaning.

$$\chi = \frac{Ng^2\mu_B{}^2}{4kT}\left[\frac{A}{B}\right]^{2/3} \tag{1}$$

where

$$A = 1.0 + 5.7979916y + 16.902653y^2 + 29.376885y^3 + 29.832959y^4 + 14.036918y^5$$

$$B = 1.0 + 2.7979916y + 7.0086780y^2 + 8.653644y^3 + 4.5743114y^4$$

and

$$y = J/2kT$$

A molecular field correction has been considered in the mean-field approximation with zj' as the magnetic interaction between chains.[11]

$$\chi_m = \frac{\chi}{1 - \chi(2zj'/Ng^2\mu_B{}^2)}$$

The following best fit parameters for **1** were obtained: $2J/k = +56.8$ K, $2zj'/k = -0.91$ K, and $g = 2.00$. The calculated

(10) Baker, G. A.; Rushbrooke, G. S. J.; Gillbert, H. E. *Phys. Rev.* **1964**, *135A*, 1272.
(11) Myers, B. E.; Berger, L.; Friedberg, S. A. *J. Appl. Phys.* **1968**, *40*, 1149.

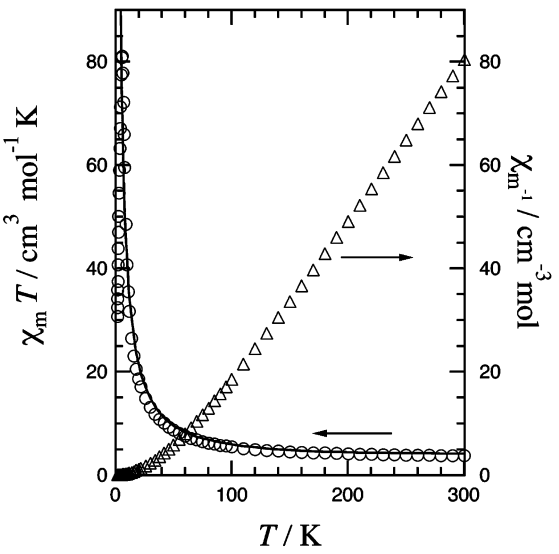

Figure 5. Temperature dependence of the product $\chi_m T$ (O) and χ_m^{-1} (△) measured at 500 Oe for [Mn(hfac)$_2$hin] (**2**). Solid line represents the theoretical curve based on the Seiden ferrimagnetic chain model.

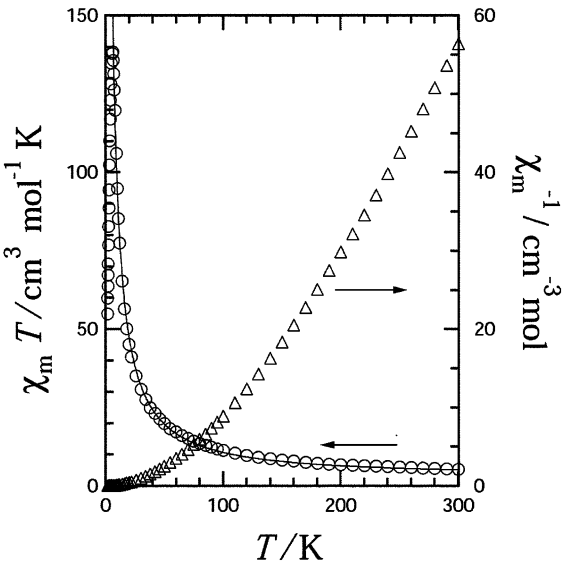

Figure 6. Temperature dependence of the product $\chi_m T$ (○) and χ_m^{-1} (△) measured at 500 Oe for [Mn(hfac)$_2$hnn] (**3**). Solid line represents the theoretical curve based on the Seiden ferrimagnetic chain model.

curve is superimposed in Figure 3. The final drop of the $\chi_m T$ value below 2.8 K is attributed also to a saturation effect of magnetization, and j' was somewhat overestimated. The $2J/k$ value for **1** is larger than that for [Cu(hfac)$_2$menn] (+36.9 K, menn = 2,4,4,5,5-pentamethylimidazoline-1-oxyl 3-oxide),[12] which shows ferromagnetic interaction between the Cu ion and radical spin. This result suggests that the hin ligands can be useful for achieving the strong exchange interaction.

The temperature dependences of $\chi_m T$ and χ_m^{-1} measured at 500 Oe for manganese(II) complexes **2** and **3** are shown in Figures 5 and 6, respectively. The $\chi_m T$ value of **2** at 300 K (3.73 cm^3 mol^{-1} K) is smaller than the calculated value of 4.75 cm^3 mol^{-1} K for a noncoupled system. This finding indicates that ferrimagnetic interaction is operative in **2**. On the other hand, the $\chi_m T$ value of **3** at 300 K (5.3 cm^3 mol^{-1} K) is larger than that of a noncoupled system. Only from this result we cannot tell whether the interaction of **3** is ferromagnetic or ferrimagnetic, but a quantitative analysis based on a ferromagnetic model gave unsatisfactory results. We assume that a broad minimum characteristic of ferrimagnetic systems appears at ca. 300 K for **2** and at a temperature much higher than 300 K for **3**.

Upon cooling, the $\chi_m T$ values increased to a maximum value 81.0 cm^3 mol^{-1} K at 6 K for **2** and 139 cm^3 mol^{-1} K at 6 K for **3** and then decreased. The maximum values are much larger than that of $S = 2$ (3.0 cm^3 mol^{-1} K) due to an antiferromagnetically correlated unit for **2** and **3**. This magnetic behavior indicates that ferrimagnetic interaction is operative infinitely along the chain structures. We analyzed the experimental data according to Seiden's ferrimagnetic chain model[13] (eq 2). Here, the definition of δ and Λ as a function of JS/kT is described in the literature.[13,14] In the case of **3**, an averaged parameter J is applied though there are two independent chains. The small letter s and capital letter S refer to the spin of $^1/_2$ (hin) and spin of $^5/_2$ (Mn^{II}), respectively. A purity factor α was introduced, and the g-value was fixed to be 2.00. The best fit parameter is $2J/k$ = −325 K for **2** and −740 K for **3**. The estimated purities are 90% for **2** and 100% for **3**, suggesting the presence of solvent or decomposed diamagnetic impurity in the specimen of **2**.

$$\chi_m = \alpha\frac{N\mu_B^2}{3kT}\left[g_s^2S^2\left(\frac{S+1}{S}+\frac{2\delta}{1-\delta}\right)-4g_Sg_s\Lambda sS\frac{1}{1-\delta}+ g_s^2\left(s(s+1)+2\Lambda^2s^2\frac{1}{1-\delta}\right)\right] \quad (2)$$

The $M-H$ curves of **1** and **2** measured at 1.8 K are shown in Figure 7. The saturation magnetizations of 11000 and 21000 erg Oe^{-1} mol^{-1} for **1** and **2**, respectively, correspond to the values of $S = 1$ and $S = 2$ with $g = 2$, supporting the presence of strong ferro- and antiferromagnetic couplings between metal and radical spins, respectively. Furthermore, the experimental data exceeded the theoretical Brillouin functions, and the ferro- and ferrimagnetic chain structures

(12) Caneschi, A.; Gatteschi, D.; Laugier, J.; Rey, P. *J. Am. Chem. Soc.* **1987**, *109*, 2191. Cabello, C. I.; Caneschi, A.; Carlin, R. L.; Gatteschi, D.; Rey, P.; Sessoli, R. *Inorg. Chem.* **1990**, *29*, 2582.

(13) Seiden, J. *J. Phys. (Paris) Lett.* **1983**, *44*, L947.

(14)

$$\gamma = -JS/2kT$$

$$a_0 = 4\left[\gamma^{-1}\sinh\gamma - \gamma^{-2}\cosh\gamma + \gamma^{-2}\right]$$

$$a_1 = 12\left[\left(\gamma^{-1}+12\gamma^{-3}\right)\sinh\gamma - \left(5\gamma^{-2}+12\gamma^{-4}\right)\cosh\gamma - \gamma^{-2}+12\gamma^{-4}\right]$$

$$b_0 = \gamma^{-1}\left(\cosh\gamma - 1\right)$$

$$b_1 = 3\left[\left(\gamma^{-1}+4\gamma^{-3}\right)\cosh\gamma - 4\gamma^{-2}\sinh\gamma + \gamma^{-1} - 4\gamma^{-3}\right]$$

$$\delta = \frac{a_1}{3a_0}, \quad \Lambda = 2\left[\frac{b_1}{3a_0}+\frac{b_0}{a_0}\right]$$

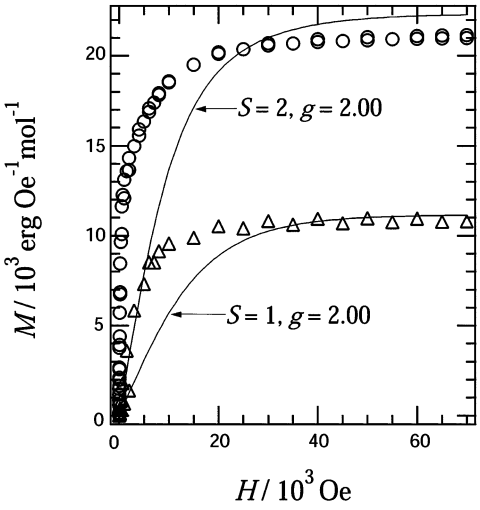

Figure 7. Field dependence of the magnetization of [Cu(hfac)$_2$hin] (**1**; △) and [Mn(hfac)$_2$hin] (**2**; ○) measured at 1.8 K. Solid lines correspond to the theoretical Brillouin functions of $S = 1$ and 2.

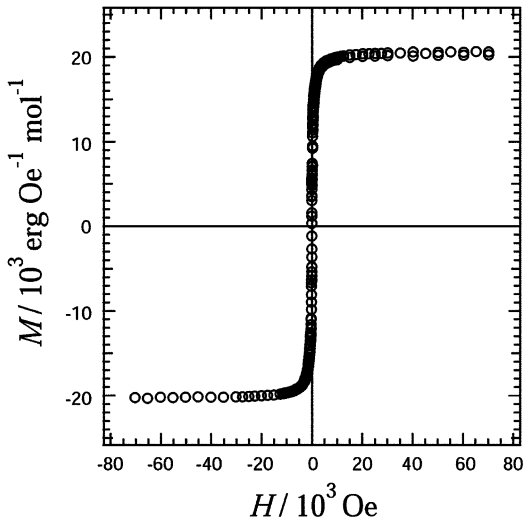

Figure 8. Field dependence of the magnetization of [Mn(hfac)$_2$hnn] (**3**) measured at 1.8 K.

are confirmed for **1** and **2**, respectively. In the case of **2**, the saturation magnetization is slightly smaller than the theoretical value of $S = 2$ and $g = 2$ (22300 erg Oe^{-1} mol^{-1}). The purity was estimated to be 94%, in accordance with the result of the temperature dependence of $\chi_m T$. No bulk magnetic ordering was observed down to 1.8 K. This paramagnetic behavior is rationalized by the one-dimensional character of **1** and **2**.

The $M-H$ curves of **3** measured at 1.8 K are shown in Figure 8. The saturation magnetizations of 21000 erg Oe^{-1} mol^{-1} correspond to the values of $S = 2$ with $g = 2.0$, supporting the antiferromagnetic couplings between Mn^{II} and radical spins like **2**. The magnetization curve of **3** measured at 1.8 K shows a very small hysteresis behavior with the coercive field of ca. 30 Oe. This finding indicates that bulk magnetic ordering took place above 1.8 K. In order to determine the magnetic phase transition temperature (T_N), we measured field-cooled magnetization, remnant magnetization, and zero-field-cooled magnetization for **3** (Figure 9a). The T_N was defined to be 4.4 K where the RM disappeared

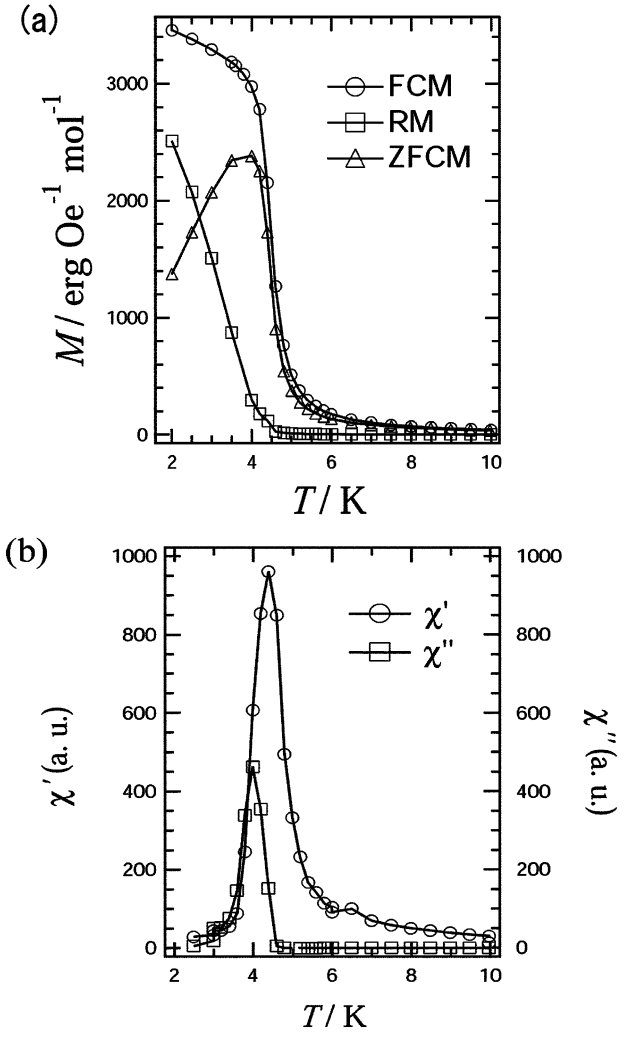

Figure 9. (a) Field-cooled magnetization (FCM), remnant magnetization (RM), and zero-field-cooled magnetization (ZFCM) of [Mn(hfac)$_2$hnn] (**3**) measured at 5, 0, and 5 Oe, respectively. (b) Temperature dependence of the in-phase (χ') and out-of-phase (χ'') components of the ac susceptibility of **3** (ac magnetic field: amplitude, 5 Oe; frequency, 10000 Hz). Solid lines are drawn as a guide to the eye.

completely on warming. The alternating current (ac) magnetic susceptibility of **3** was measured in the ac field amplitude of 5 Oe oscillating at 10000 Hz in a temperature range 10−2 K (Figure 9b). The peak of the real component (χ') at 4.4 K is noticeable. This behavior implies that the long-range magnetic ordering occurs at $T_N = 4.4$ K. We observed no frequency dependence of the real or imaginary part of the ac susceptibility for **3**.

Discussion

We have described the crystal structure of **1**, which is the first example of an infinite chain complex containing the hin bridge. The ferromagnetic interaction of **1** can be explained in terms of orbital orthogonality between the copper $3d_{x^2-y^2}$ and the oxygen or nitrogen $2p_z$ orbitals, as often discussed in Cu(hfac)$_2$ nitronyl nitroxide complexes.[12] On the other hand, the antiferromagnetic interaction of **2** and **3** can be attributed to orbital overlap between the manganese $3d_{xz}$ and $3d_{yz}$ and the oxygen or nitrogen $2p_z$ orbitals, like

$Mn(hfac)_2$ nitronyl nitroxide complexes.[15] Such ferro- and antiferromagnetic couplings have been widely observed in metal−oxygen coordination bonds in nitronyl nitroxide complexes. In the present study, a similar argument can also be applied to the coordinating metal−nitrogen bonds in the hin complexes.

Interestingly, the magnetic exchange couplings between metal and hin spins in **1** ($2J/k = +56.8$ K) are larger than those of the corresponding nitronyl nitroxide derivatives ([$Cu(hfac)_2$Rnn]: $2J/k = +36.9$ and $+30.8$ K (R = methyl and isopropyl, respectively)).[12] Strong interaction can be expected in less bulky systems in general, and the present results are ascribable especially to the choice of the smallest ligands in the nitronyl nitroxide and imino nitroxide families. For more detailed discussion, we have to think of several features based on geometrical and electronic structures of **1**. The bond distances of Cu−N2 and Cu−O3 are comparable to or slightly shorter than the typical values of Cu−O for nitronyl nitroxide complexes (e.g.: [$Cu(hfac)_2$Rnn], 2.341(6) and 2.431(5) Å for R = methyl,[12] 2.407(6) and 2.446(8) Å for R = isopropyl;[12] [{$Cu(hfac)_2(H_2O)$}$_2$(μ-hnn)],[5] 2.462(2) Å). However, the slight difference of the bond lengths alone can hardly account for the large exchange interaction of **1**.

As McConnell has pointed out, the exchange coupling is proportional to the spin densities on the interacting atoms ($H^{AB} = -S^A \cdot S^B \sum J_{ij} \rho_i^A \rho_j^B$),[16] and accordingly the higher spin densities on the terminal atoms (N and O) of the ONCN group than those of the ONCNO group may afford stronger exchange interactions. We have no experimental evidence of the spin distribution in hin and hnn. The spin distributions in hin and hnn can be estimated by means of semiempirical calculation methods. We carried out UHF/PM3[17] calculations using the geometries determined by the X-ray crystallographic analysis; the atomic coordinates of hnn and hin were available from the hnn moiety in [{$Cu(hfac)_2(H_2O)$}$_2$(μ-hnn)][5] and the hin moiety in [$Cu(hfac)_2$hin]. The calculated spin densities are $\rho(O) = 0.323$ for hnn and $\rho(O) = 0.429$ and $\rho(N_{terminal}) = 0.376$ for hin. The higher spin densities in hin are responsible for the stronger ferromagnetic interactions in comparison to those of the hnn complexes.

In the case of manganese(II) complexes, the magnitude of the exchange interaction of **2** ($2J/k = -325$ K) is comparable to those of other nitronyl nitroxide derivatives ([$Mn(hfac)_2$Rnn]: $2J/k = -471$, -371, -310, and -297 K (R = isopropyl, ethyl, methyl, and phenyl, respectively)).[15] However, the exchange interaction of **2** is much weaker than that of **3** ($2J/k = -740$ K) probably because of stronger chemical affinity of Mn−O than that of Mn−N. Indeed the bond lengths between manganese and nitroxide oxygen are shorter than those of manganese and imino nitroxide nitrogen. Unfortunately we could not determine the crystal structure of **2**, and we compare the bond lengths between **3** and a prototype compound [$Mn(hfac)_2(hin)_2$];[5] 2.139(4), 2.142(4), 2.129(4), and 2.139(4) Å for the Mn−O(hnn) bonds vs 2.208(3) and 2.224(3) Å for the Mn−N(hin) bonds. The shorter Mn(II)−O bond lengths bring about the stronger exchange interactions between Mn(II) and radical spins. Therefore, the advantage of the higher spin density at the $N_{terminal}$ atom in hin is canceled out by the long Mn−N bond in **3**.

Nevertheless, we can stress that hnn is a promising ligand for development of strongly correlated ferrimagnetic systems, as demonstrated by the considerably large intrachain interaction in [$Mn(hfac)_2$hnn] (**3**). The hin ligand is also a good candidate for constructing copper(II)-based magnetic systems such as [$Cu(hfac)_2$hin] (**1**), although it seems to be less useful in constructing manganese(II)-based magnetic systems.

The mechanism of the three-dimensional magnetic order of **3** can be understood similarly to the system of [$Mn(hfac)_2$Rnn] (R = isopropyl, *n*-propyl, and ethyl) reported by Gatteschi.[15] The T_N for **3** (4.6 K) is lower, while the magnitude of exchange interaction of **3** ($2J/k = -740$ K) is much stronger than those of other nitronyl nitroxide derivatives ([$Mn(hfac)_2$Rnn]: $T_N = 8.1$ and 8.6 K; $2J/k = -371$ and -361 K (R = ethyl and *n*-propyl, respectively)). Reasons for the low T_N of **3** are not clear so far. The transition temperatures generally depend not only on the intrachain interaction but also on the interchain ones. Owing to the smaller substituent in **3** than those in [$Mn(hfac)_2$Rnn] derivatives, the interchain Mn···Mn distances in **3** are shorter than those in the latter; 8.35−11.3 Å for **3** and 8.89−12.11 Å for [$Mn(hfac)_2$Rnn] (R = ethyl and *n*-propyl). We can hardly explain that the longer interchain distances bring about the higher T_N, but only point out the similar distance dependence of the transition temperatures of layered magnets reported by Drillon, Awaga, and their co-workers.[18] They proposed the through-space dipolar interaction between the layers to interpret the unexpected finding of the high T_N related with the large spacing. Preliminary results of the magnetic measurements on a single crystal of **3** suggest that the easy magnetization axis lies along the chain direction. In this situation antiparallel alignment of the classical magnetic moments is preferable, and the shorter distance between the chains is unfavorable for parallel moment alignment, presumably giving the lower T_N.

Summary

We have demonstrated the one-dimensional magnetic properties of [$Cu(hfac)_2$hin] and [$Mn(hfac)_2$hin]. They are the first examples of the hin−metal complexes with one-dimensional magnetic structures. Relatively strong magnetic couplings, especially in the copper(II) complex, were found in the hin complexes compared with the conventional Rnn

(15) Caneschi, A.; Gatteschi, D.; Renard, J. P.; Rey, P.; Sessoli, R. *Inorg. Chem.* **1989**, *28*, 3314. Caneschi, A.; Gatteschi, D.; Lalioti, N.; Sangregorio, C.; Sessoli, R. *J. Chem. Soc., Dalton Trans.* **2000**, 3907. Caneschi, A.; Gatteschi, D.; Rey, P.; Sessoli, R. *Inorg. Chem.* **1988**, *27*, 1756.
(16) McConnell, H. M. *J. Chem. Phys*. **1963**, *39*, 1910.
(17) Stewart, J. J. P. *MOPAC 97*; Fujitsu Ltd: Tokyo, Japan, 1997.
(18) Rabu, R.; Rouba, S.; Laget, V.; Hornic, C.; Drillon, M. *Chem. Commun*. **1996**, 1107. Laget, V.; Rouba, S.; Hornic, C.; Drillon, M. *J. Magn. Magn. Mater*. **1996**, *154*, L7. Laget, V.; Hornic, C.; Rabu, P.; Drillon, M.; Ziessel, R. *Cood. Chem. Rev.* **1998**, *178−180*, 1533. Fujita, W.; Awaga, K. *Inorg. Chem*. **1996**, *35*, 1915. Fujita, W.; Awaga, K. *J. Am. Chem. Soc*. **1997**, *119*, 4563. Girtu, M. A.; Wynn, C. M.; Fujita, W.; Awaga, K.; Epstein, A. J. *Phys. Rev. B* **1998**, *57*, 11058. Hornick, C.; Rabu, P.; Drillon, M. *Polyhedron* **2000**, *19*, 259.

complexes. Furthermore, we also found that, even when the hnn is available, it can be useful in pursuit of strongly correlated magnetic materials using manganese(II) ions.

Recently Gatteschi and co-workers reported that polymeric $M(hfac)_2$−nitronyl nitroxide systems were potentially good candidates for single-molecule magnets.[19] Slow magnetic relaxation in one-dimensional magnets requires the condition that the ratio of the intrachain interaction over the interchain interaction must be high.[19] The stronger intrachain interactions across the hin bridge than those across nitronyl nitroxide bridges may satisfy this requirement. Preparation of polymeric complexes using hin with other metal ions having large single-ion anisotropy such as cobalt(II) ions in place of copper(II) and manganese(II) is currently underway.

Acknowledgment. This work was supported by Grants-in-Aid for Scientific Research on Priority Areas (No. 730/11224204 and 401/11136212) from the Ministry of Education, Culture, Sports, Science and Technology, Japan.

Supporting Information Available: Crystallographic data (excluding structure factors) for the structures of **1** and **3** in CIF format. This material is available free of charge via the Internet at http://pubs.acs.org.

IC034392X

(19) Caneschi, A.; Gatteschi, D.; Lalioti, N.; Sangregorio, C.; Sessoli, R.; Venturi, G.; Vindigni, A.; Rettori, A.; Pini, M. G.; Novak, M. A. *Angew. Chem., Int. Ed.* **2001**, *40*, 1760